

Search for GeV-scale dark matter annihilation in the Sun with IceCube DeepCore

R. Abbasi,¹⁷ M. Ackermann,⁶⁰ J. Adams,¹⁸ J. A. Aguilar,¹² M. Ahlers,²² M. Ahrens,⁵¹ J. M. Alameddine,²³ C. Alispach,²⁸ A. A. Alves, Jr.,³¹ N. M. Amin,⁴³ K. Andeen,⁴¹ T. Anderson,⁵⁷ G. Anton,²⁶ C. Argüelles,¹⁴ Y. Ashida,³⁹ S. Axani,¹⁵ X. Bai,⁴⁷ A. Balagopal,³⁹ A. Barbano,²⁸ S. W. Barwick,³⁰ B. Bastian,⁶⁰ V. Basu,³⁹ S. Baur,¹² R. Bay,⁸ J. J. Beatty,^{20,21} K.-H. Becker,⁵⁹ J. Becker Tjus,¹¹ C. Bellenghi,²⁷ S. BenZvi,⁴⁹ D. Berley,¹⁹ E. Bernardini,^{60,*} D. Z. Besson,^{34,†} G. Binder,^{8,9} D. Bindig,⁵⁹ E. Blaufuss,¹⁹ S. Blot,⁶⁰ M. Boddenberg,¹ F. Bontempo,³¹ J. Borowka,¹ S. Böser,⁴⁰ O. Botner,⁵⁸ J. Böttcher,¹ E. Bourbeau,²² F. Bradascio,⁶⁰ J. Braun,³⁹ B. Brinson,⁶ S. Bron,²⁸ J. Brostean-Kaiser,⁶⁰ S. Browne,³² A. Burgman,⁵⁸ R. T. Burley,² R. S. Busse,⁴² M. A. Campana,⁴⁶ E. G. Carnie-Bronca,² C. Chen,⁶ Z. Chen,⁵² D. Chirkin,³⁹ K. Choi,⁵³ B. A. Clark,²⁴ K. Clark,³³ L. Classen,⁴² A. Coleman,⁴³ G. H. Collin,¹⁵ J. M. Conrad,¹⁵ P. Coppin,¹³ P. Correa,¹³ D. F. Cowen,^{56,57} R. Cross,⁴⁹ C. Dappen,¹ P. Dave,⁶ C. De Clercq,¹³ J. J. DeLaunay,⁵⁵ D. Delgado López,¹⁴ H. Dembinski,⁴³ K. Deoskar,⁵¹ A. Desai,³⁹ P. Desiati,³⁹ K. D. de Vries,¹³ G. de Wasseige,³⁶ M. de With,¹⁰ T. DeYoung,²⁴ A. Diaz,¹⁵ J. C. Díaz-Vélez,³⁹ M. Dittmer,⁴² H. Dujmovic,³¹ M. Dunkman,⁵⁷ M. A. DuVernois,³⁹ E. Dvorak,⁴⁷ T. Ehrhardt,⁴⁰ P. Eller,²⁷ R. Engel,^{31,32} H. Erpenbeck,¹ J. Evans,¹⁹ P. A. Evenson,⁴³ K. L. Fan,¹⁹ A. R. Fazely,⁷ N. Feigl,¹⁰ S. Fiedlschuster,²⁶ A. T. Fienberg,⁵⁷ K. Filimonov,⁸ C. Finley,⁵¹ L. Fischer,⁶⁰ D. Fox,⁵⁶ A. Franckowiak,^{11,60} E. Friedman,¹⁹ A. Fritz,⁴⁰ P. Fürst,¹ T. K. Gaisser,⁴³ J. Gallagher,³⁸ E. Ganster,¹ A. Garcia,¹⁴ S. Garrappa,⁶⁰ L. Gerhardt,⁹ A. Ghadimi,⁵⁵ C. Glaser,⁵⁸ T. Glauch,²⁷ T. Glüsenskamp,²⁶ J. G. Gonzalez,⁴³ S. Goswami,⁵⁵ D. Grant,²⁴ T. Grégoire,⁵⁷ S. Griswold,⁴⁹ C. Günther,¹ P. Gutjahr,²³ C. Haack,²⁷ A. Hallgren,⁵⁸ R. Halliday,²⁴ L. Halve,¹ F. Halzen,³⁹ M. Ha Minh,²⁷ K. Hanson,³⁹ J. Hardin,³⁹ A. A. Harnisch,²⁴ A. Haungs,³¹ D. Hebecker,¹⁰ K. Helbing,⁵⁹ F. Henningsen,²⁷ E. C. Hetteringer,²⁴ S. Hickford,⁵⁹ J. Hignight,²⁵ C. Hill,¹⁶ G. C. Hill,² K. D. Hoffman,¹⁹ R. Hoffmann,⁵⁹ B. Hokanson-Fasig,³⁹ K. Hoshina,^{39,‡} F. Huang,⁵⁷ M. Huber,²⁷ T. Huber,³¹ K. Hultqvist,⁵¹ M. Hünnefeld,²³ R. Hussain,³⁹ K. Hymon,²³ S. In,⁵³ N. Iovine,¹² A. Ishihara,¹⁶ M. Jansson,⁵¹ G. S. Japaridze,⁵ M. Jeong,⁵³ M. Jin,¹⁴ B. J. P. Jones,⁴ D. Kang,³¹ W. Kang,⁵³ X. Kang,⁴⁶ A. Kappes,⁴² D. Kappesser,⁴⁰ L. Kardum,²³ T. Karg,⁶⁰ M. Karl,²⁷ A. Karle,³⁹ U. Katz,²⁶ M. Kauer,³⁹ M. Kellermann,¹ J. L. Kelley,³⁹ A. Kheirandish,⁵⁷ K. Kin,¹⁶ T. Kintscher,⁶⁰ J. Kiryluk,⁵² S. R. Klein,^{8,9} R. Koirala,⁴³ H. Kolanoski,¹⁰ T. Kontrimas,²⁷ L. Köpke,⁴⁰ C. Kopper,²⁴ S. Kopper,⁵⁵ D. J. Koskinen,²² P. Koundal,³¹ M. Kovacevich,⁴⁶ M. Kowalski,^{10,60} T. Kozynets,²² E. Kun,¹¹ N. Kurahashi,⁴⁶ N. Lad,⁶⁰ C. Lagunas Gualda,⁶⁰ J. L. Lanfranchi,⁵⁷ M. J. Larson,¹⁹ F. Lauber,⁵⁹ J. P. Lazar,^{14,39} J. W. Lee,⁵³ K. Leonard,³⁹ A. Leszczyńska,³² Y. Li,⁵⁷ M. Lincetto,¹¹ Q. R. Liu,³⁹ M. Liubarska,²⁵ E. Lohfink,⁴⁰ C. J. Lozano Mariscal,⁴² L. Lu,³⁹ F. Lucarelli,²⁸ A. Ludwig,^{24,35} W. Luszczak,³⁹ Y. Lyu,^{8,9} W. Y. Ma,⁶⁰ J. Madsen,³⁹ K. B. M. Mahn,²⁴ Y. Makino,³⁹ S. Mancina,³⁹ I. C. Mariş,¹² I. Martinez-Soler,¹⁴ R. Maruyama,⁴⁴ K. Mase,¹⁶ T. McElroy,²⁵ F. McNally,³⁷ J. V. Mead,²² K. Meagher,³⁹ S. Mechbal,⁶⁰ A. Medina,²¹ M. Meier,¹⁶ S. Meighen-Berger,²⁷ J. Micallef,²⁴ D. Mockler,¹² T. Montaruli,²⁸ R. W. Moore,²⁵ R. Morse,³⁹ M. Moulai,¹⁵ R. Naab,⁶⁰ R. Nagai,¹⁶ U. Naumann,⁵⁹ J. Necker,⁶⁰ G. Neer,²⁴ L. V. Nguyẽn,²⁴ H. Niederhausen,²⁴ M. U. Nisa,²⁴ S. C. Nowicki,²⁴ A. Obertacke Pollmann,⁵⁹ M. Oehler,³¹ B. Oeyen,²⁹ A. Olivas,¹⁹ E. O'Sullivan,⁵⁸ H. Pandya,⁴³ D. V. Pankova,⁵⁷ N. Park,³³ G. K. Parker,⁴ E. N. Paudel,⁴³ L. Paul,⁴¹ C. Pérez de los Heros,⁵⁸ L. Peters,¹ J. Peterson,³⁹ S. Philippen,¹ S. Pieper,⁵⁹ M. Pittermann,³² A. Pizzuto,³⁹ M. Plum,⁴¹ Y. Popovych,⁴⁰ A. Porcelli,²⁹ M. Prado Rodriguez,³⁹ P. B. Price,⁸ B. Pries,²⁴ G. T. Przybylski,⁹ C. Raab,¹² A. Raissi,¹⁸ M. Rameez,²² K. Rawlins,³ I. C. Rea,²⁷ A. Rehman,⁴³ P. Reichherzer,¹¹ R. Reimann,¹ G. Renzi,¹² E. Resconi,²⁷ S. Reusch,⁶⁰ W. Rhode,²³ M. Richman,⁴⁶ B. Riedel,³⁹ E. J. Roberts,² S. Robertson,^{8,9} G. Roellinghoff,⁵³ M. Rongen,⁴⁰ C. Rott,^{50,53} T. Ruhe,²³ D. Ryckbosch,²⁹ D. Rysewyk Cantu,²⁴ I. Safa,^{14,39} J. Saffer,³² S. E. Sanchez Herrera,²⁴ A. Sandrock,²³ J. Sandroos,⁴⁰ M. Santander,⁵⁵ S. Sarkar,⁴⁵ S. Sarkar,²⁵ K. Satalecka,⁶⁰ M. Schaufel,¹ H. Schieler,³¹ S. Schindler,²⁶ T. Schmidt,¹⁹ A. Schneider,³⁹ J. Schneider,²⁶ F. G. Schröder,^{31,43} L. Schumacher,²⁷ G. Schwefer,¹ S. Sclafani,⁴⁶ D. Seckel,⁴³ S. Seunarine,⁴⁸ A. Sharma,⁵⁸ S. Shefali,³² M. Silva,³⁹ B. Skrzypek,¹⁴ B. Smithers,⁴ R. Snihur,³⁹ J. Soedingrekso,²³ D. Soldin,⁴³ C. Spannfellner,²⁷ G. M. Spiczak,⁴⁸ C. Spiering,^{60,†} J. Stachurska,⁶⁰ M. Stamatikos,²¹ T. Stanev,⁴³ R. Stein,⁶⁰ J. Stettner,¹ A. Steuer,⁴⁰ T. Stezelberger,⁹ T. Stürwald,⁵⁹ T. Stuttard,²² G. W. Sullivan,¹⁹ I. Taboada,⁶ S. Ter-Antonyan,⁷ S. Tilav,⁴³ F. Tischbein,¹ K. Tollefson,²⁴ C. Tönnes,⁵⁴ S. Toscano,¹² D. Tosi,³⁹ A. Tretin,⁶⁰ M. Tselengidou,²⁶ C. F. Tung,⁶ A. Turcati,²⁷ R. Turcotte,³¹ C. F. Turley,⁵⁷ J. P. Twagirayezu,²⁴ B. Ty,³⁹ M. A. Unland Elorrieta,⁴² N. Valtonen-Mattila,⁵⁸ J. Vandenbroucke,³⁹ N. van Eijndhoven,¹³ D. Vannerom,¹⁵ J. van Santen,⁶⁰ S. Verpoest,²⁹ C. Walck,⁵¹ T. B. Watson,⁴ C. Weaver,²⁴ P. Weigel,¹⁵ A. Weindl,³¹ M. J. Weiss,⁵⁷ J. Weldert,⁴⁰ C. Wendt,³⁹ J. Werthebach,²³ M. Weyrauch,³² N. Whitehorn,^{24,35} C. H. Wiebusch,¹ D. R. Williams,⁵⁵ M. Wolf,²⁷ K. Woschnagg,⁸ G. Wrede,²⁶ J. Wulff,¹¹ X. W. Xu,⁷ J. P. Yanez,²⁵ S. Yoshida,¹⁶ S. Yu,²⁴ T. Yuan,³⁹ Z. Zhang,⁵² and P. Zhelmin¹⁴

(IceCube Collaboration)

- ¹*III. Physikalisches Institut, RWTH Aachen University, D-52056 Aachen, Germany*
- ²*Department of Physics, University of Adelaide, Adelaide 5005, Australia*
- ³*Department of Physics and Astronomy, University of Alaska Anchorage, 3211 Providence Drive, Anchorage, Alaska 99508, USA*
- ⁴*Department of Physics, University of Texas at Arlington, 502 Yates Street, Science Hall Rm 108, Box 19059, Arlington, Texas 76019, USA*
- ⁵*CTSPS, Clark-Atlanta University, Atlanta, Georgia 30314, USA*
- ⁶*School of Physics and Center for Relativistic Astrophysics, Georgia Institute of Technology, Atlanta, Georgia 30332, USA*
- ⁷*Department of Physics, Southern University, Baton Rouge, Louisiana 70813, USA*
- ⁸*Department of Physics, University of California, Berkeley, California 94720, USA*
- ⁹*Lawrence Berkeley National Laboratory, Berkeley, California 94720, USA*
- ¹⁰*Institut für Physik, Humboldt-Universität zu Berlin, D-12489 Berlin, Germany*
- ¹¹*Fakultät für Physik & Astronomie, Ruhr-Universität Bochum, D-44780 Bochum, Germany*
- ¹²*Université Libre de Bruxelles, Science Faculty CP230, B-1050 Brussels, Belgium*
- ¹³*Vrije Universiteit Brussel (VUB), Dienst ELEM, B-1050 Brussels, Belgium*
- ¹⁴*Department of Physics and Laboratory for Particle Physics and Cosmology, Harvard University, Cambridge, Massachusetts 02138, USA*
- ¹⁵*Department of Physics, Massachusetts Institute of Technology, Cambridge, Massachusetts 02139, USA*
- ¹⁶*Department of Physics and Institute for Global Prominent Research, Chiba University, Chiba 263-8522, Japan*
- ¹⁷*Department of Physics, Loyola University Chicago, Chicago, Illinois 60660, USA*
- ¹⁸*Department of Physics and Astronomy, University of Canterbury, Private Bag 4800, Christchurch, New Zealand*
- ¹⁹*Department of Physics, University of Maryland, College Park, Maryland 20742, USA*
- ²⁰*Department of Astronomy, Ohio State University, Columbus, Ohio 43210, USA*
- ²¹*Department of Physics and Center for Cosmology and Astro-Particle Physics, Ohio State University, Columbus, Ohio 43210, USA*
- ²²*Niels Bohr Institute, University of Copenhagen, DK-2100 Copenhagen, Denmark*
- ²³*Department of Physics, TU Dortmund University, D-44221 Dortmund, Germany*
- ²⁴*Department of Physics and Astronomy, Michigan State University, East Lansing, Michigan 48824, USA*
- ²⁵*Department of Physics, University of Alberta, Edmonton, Alberta T6G 2E1, Canada*
- ²⁶*Erlangen Centre for Astroparticle Physics, Friedrich-Alexander-Universität Erlangen-Nürnberg, D-91058 Erlangen, Germany*
- ²⁷*Physik-department, Technische Universität München, D-85748 Garching, Germany*
- ²⁸*Département de physique nucléaire et corpusculaire, Université de Genève, CH-1211 Genève, Switzerland*
- ²⁹*Department of Physics and Astronomy, University of Gent, B-9000 Gent, Belgium*
- ³⁰*Department of Physics and Astronomy, University of California, Irvine, California 92697, USA*
- ³¹*Karlsruhe Institute of Technology, Institute for Astroparticle Physics, D-76021 Karlsruhe, Germany*
- ³²*Karlsruhe Institute of Technology, Institute of Experimental Particle Physics, D-76021 Karlsruhe, Germany*
- ³³*Department of Physics, Engineering Physics, and Astronomy, Queen's University, Kingston, Ontario K7L 3N6, Canada*
- ³⁴*Department of Physics and Astronomy, University of Kansas, Lawrence, Kansas 66045, USA*
- ³⁵*Department of Physics and Astronomy, UCLA, Los Angeles, California 90095, USA*
- ³⁶*Centre for Cosmology, Particle Physics and Phenomenology—CP3, Université catholique de Louvain, Louvain-la-Neuve, Belgium*
- ³⁷*Department of Physics, Mercer University, Macon, Georgia 31207-0001, USA*
- ³⁸*Department of Astronomy, University of Wisconsin—Madison, Madison, Wisconsin 53706, USA*
- ³⁹*Department of Physics and Wisconsin IceCube Particle Astrophysics Center, University of Wisconsin—Madison, Madison, Wisconsin 53706, USA*
- ⁴⁰*Institute of Physics, University of Mainz, Staudinger Weg 7, D-55099 Mainz, Germany*
- ⁴¹*Department of Physics, Marquette University, Milwaukee, Wisconsin 53201, USA*
- ⁴²*Institut für Kernphysik, Westfälische Wilhelms-Universität Münster, D-48149 Münster, Germany*
- ⁴³*Bartol Research Institute and Department of Physics and Astronomy, University of Delaware, Newark, Delaware 19716, USA*

⁴⁴*Department of Physics, Yale University, New Haven, Connecticut 06520, USA*⁴⁵*Department of Physics, University of Oxford, Parks Road, Oxford OX1 3PU, United Kingdom*⁴⁶*Department of Physics, Drexel University, 3141 Chestnut Street, Philadelphia, Pennsylvania 19104, USA*⁴⁷*Physics Department, South Dakota School of Mines and Technology, Rapid City, South Dakota 57701, USA*⁴⁸*Department of Physics, University of Wisconsin, River Falls, Wisconsin 54022, USA*⁴⁹*Department of Physics and Astronomy, University of Rochester, Rochester, New York 14627, USA*⁵⁰*Department of Physics and Astronomy, University of Utah, Salt Lake City, Utah 84112, USA*⁵¹*Oskar Klein Centre and Department of Physics, Stockholm University, SE-10691 Stockholm, Sweden*⁵²*Department of Physics and Astronomy, Stony Brook University, Stony Brook, New York 11794-3800, USA*⁵³*Department of Physics, Sungkyunkwan University, Suwon 16419, Korea*⁵⁴*Institute of Basic Science, Sungkyunkwan University, Suwon 16419, Korea*⁵⁵*Department of Physics and Astronomy, University of Alabama, Tuscaloosa, Alabama 35487, USA*⁵⁶*Department of Astronomy and Astrophysics, Pennsylvania State University, University Park, Pennsylvania 16802, USA*⁵⁷*Department of Physics, Pennsylvania State University, University Park, Pennsylvania 16802, USA*⁵⁸*Department of Physics and Astronomy, Uppsala University, Box 516, S-75120 Uppsala, Sweden*⁵⁹*Department of Physics, University of Wuppertal, D-42119 Wuppertal, Germany*⁶⁰*DESY, D-15738 Zeuthen, Germany*

(Received 18 November 2021; accepted 7 February 2022; published 21 March 2022)

The Sun provides an excellent target for studying spin-dependent dark matter-proton scattering due to its high matter density and abundant hydrogen content. Dark matter particles from the Galactic halo can elastically interact with Solar nuclei, resulting in their capture and thermalization in the Sun. The captured dark matter can annihilate into Standard Model particles including an observable flux of neutrinos. We present the results of a search for low-energy (<500 GeV) neutrinos correlated with the direction of the Sun using 7 years of IceCube data. This work utilizes, for the first time, new optimized cuts to extend IceCube's sensitivity to dark matter mass down to 5 GeV. We find no significant detection of neutrinos from the Sun. Our observations exclude capture by spin-dependent dark matter-proton scattering with cross section down to a few times 10^{-41} cm², assuming there is equilibrium with annihilation into neutrinos/antineutrinos for dark matter masses between 5 GeV and 100 GeV. These are the strongest constraints at GeV energies for dark matter annihilation directly to neutrinos.

DOI: [10.1103/PhysRevD.105.062004](https://doi.org/10.1103/PhysRevD.105.062004)

I. INTRODUCTION

Based on numerous observations from cosmology and astronomy, dark matter (DM) is believed to constitute over $\sim 80\%$ of all matter in the universe [1–4]. The quest to establish the particle nature of DM is also tied to observations in high energy astrophysics, including observations in neutrinos. The search for neutrinos produced by annihilations or decays of DM is one major aspect of indirect detection of DM from astrophysical objects. The Sun is particularly well suited for such searches as it has been gravitationally capturing candidates for DM particles such as weakly interacting massive

particles (WIMPs) from the surrounding halo for its entire lifetime of 4.5 billion years [5–9]. These particles accumulate in the Sun, where they annihilate into standard model (SM) particles as their density builds up. This process provides a route to studying WIMP interactions with nucleons since there is time for equilibrium to be established between captures and annihilations [10–14].

Given the high matter density of the Sun, the only SM particles that can escape the Sun with relatively little attenuation are neutrinos [15–21]. (Secluded DM models where DM annihilation proceeds via a long-lived mediator which can decay outside the Sun into SM particles, also allow for the production of gamma rays in addition to neutrinos correlated with the direction of the Sun [21–32]). Several experiments including Super-Kamiokande [33], IceCube [34,35] and ANTARES [36,37] have looked for neutrino signatures of DM annihilation in the Sun. These searches are especially useful for probing spin-dependent DM-proton scattering cross sections, and have already

* Also at Università di Padova, I-35131 Padova, Italy.

† Also at National Research Nuclear University, Moscow Engineering Physics Institute (MEPhI), Moscow 115409, Russia.

‡ Also at Earthquake Research Institute, University of Tokyo, Bunkyo, Tokyo 113-0032, Japan.

outperformed direct detection experiments by more than an order of magnitude in terms of sensitivity. IceCube’s previously published searches using three years of data already result in the world’s best constraints on the spin-dependent scattering cross section for DM mass in the range $\mathcal{O}(100)$ GeV to 10 TeV.

Due to IceCube’s optimal sensitivity to TeV–PeV neutrinos, the detector’s probing of DM parameter space below 50 GeV has been limited up until now, while a large parameter space for GeV WIMPs remains unconstrained [38]. This work for the first time extends IceCube’s reach to 5 GeV DM masses for some of the studied annihilation channels. The paper is structured as follows. Section II describes the IceCube detector and the process of data selection used in this analysis. Section III presents the analysis, including the details of the signal and background estimation methods used. The results are discussed in Sec. IV. Section V presents our conclusions and places the results in context.

II. ICECUBE AND DEEPCORE DATA

A. Detector

The IceCube Neutrino Observatory—located at the South Pole—consists of an array of 5160 photodetectors on 86 strings embedded within 1 km³ of the Antarctic ice. Each photodetector unit—known as a digital optical module (DOM)—is a downward facing photomultiplier tube (PMT) with associated electronics enclosed within a glass vessel [39]. The typical horizontal spacing between the strings is 125 m with 60 DOMs per string. The exception are the 8 strings in the bottom-center of the array known as DeepCore, which has a geometry optimized to lower the energy threshold of IceCube [40]. A higher density of high-quantum efficiency DOMs, coupled with the outer array acting as a veto region to reject atmospheric muons makes DeepCore particularly suitable for detecting neutrinos as low as ~ 5 GeV in energy. A detailed description of the instrumentation and signal reconstruction can be found in Refs. [41,42].

B. Event selection

We use IceCube and DeepCore data collected between January 1st, 2011 and January 1st, 2018 with a total live-time of 6.75 years. The event selection and reconstruction used in this analysis follows the same methods as those used in Ref. [43]. The IceCube DOMs surrounding the DeepCore volume are used to veto atmospheric muons. This is achieved by rejecting events in which photons in a certain time-window are observed outside before they are detected in DeepCore. The photoelectrons detected within the DeepCore volume are fitted using a multidimensional likelihood to estimate the energy and direction of a neutrino event. Each event is classified as either “tracklike” or “cascadelike”, depending on whether the fit

is better described by a ν_μ charged-current (CC) interaction, or a hadronic shower with no muon resulting from neutral current interactions as well as ν_τ/ν_e CC interactions. An eleven variable boosted decision tree (BDT) is used to further reject atmospheric muons.

The two main differences in the event reconstruction with respect to that in [43] are at the final data reduction level and are discussed here. One, we no longer require that the stopping vertex of the reconstructed muon be contained within DeepCore. Two, the boosted decision tree (BDT) cut is loosened to allow additional particles in the data sample. The purpose of the aforementioned relaxed cuts is to enhance the overall number of neutrinos in the data at the cost of an increase of 13% background contamination with respect to that given in [43]. The final sample includes 192,212 events. This is also the first time that an IceCube analysis utilizes both “tracklike” and “cascadelike” events to search for dark matter. At the low energies considered in this work, tracks and cascades show negligible differences in their angular resolutions. The median angular resolution of events in this sample at 10 GeV is $\sim 35^\circ$ and improves to $\leq 5^\circ$ above 200 GeV.

III. ANALYSIS

We use an unbinned likelihood ratio method to search for neutrinos correlated with the direction of the Sun. The one-dimensional likelihood function is given by,

$$\mathcal{L}(n_s) = \prod_i^N \left(\frac{n_s}{N} S(\Psi_i) + \left(1 - \frac{n_s}{N}\right) B(\Psi_i) \right), \quad (1)$$

where n_s is the number of signal neutrino events, N is the total number of data events, Ψ_i is the angular distance between the reconstructed direction of the i th event and the direction of the Sun, $S(\Psi_i)$ is the signal probability distribution function (PDF) for the i th data event, and $B(\Psi_i)$ is the background PDF for the i th data event. Given the similar angular resolutions of tracks and cascades in this sample, the likelihood does not depend on event-topology and tracks and cascades are treated identically. We also calculate a test statistic (TS), given by twice the logarithm of the ratio of the best-fit likelihood to the null (background-only) hypothesis,

$$\text{TS} = 2 \log \frac{\mathcal{L}(\hat{n}_s)}{\mathcal{L}(n_s = 0)}, \quad (2)$$

where \hat{n}_s is the best fit value of the number of signal events. The modeling of the signal PDF from simulation and the background PDF from randomized data are described below.

A. Signal and background probabilities

1. Neutrinos from DM annihilation

We consider only DM masses higher than 5 GeV for which evaporation from the Sun is negligibly small [44,45]. Ignoring self-interactions, the number of DM particles in the Sun $N_\chi(t)$ is given by,

$$\frac{dN_\chi}{dt} = \Gamma_{\text{cap}} - K_{\text{ann}} N_\chi^2, \quad (3)$$

where Γ_{cap} is the WIMP capture rate, and the second term expresses the annihilation rate in terms of a factor K_{ann} , that accounts for the DM number density and the velocity-averaged annihilation cross section [46]. Once equilibrium has been reached between WIMP capture and annihilation rate, the capture rate and annihilation rate Γ_{ann} are related by,

$$\Gamma_{\text{cap}} = 2\Gamma_{\text{ann}}. \quad (4)$$

The factor of two accounts for the fact that every annihilation event involves two DM particles. The capture rate itself is a function of DM-proton cross section (σ_{SD} spin-dependent and σ_{SI} spin-independent). On the observable side, the neutrino/anti-neutrino flux at Earth from DM annihilation in the Sun $d\phi_\nu/dt$ is given by,

$$\frac{d\phi_\nu}{dt} = \frac{\Gamma_{\text{ann}}}{4\pi D^2} \frac{dN_\nu}{dE}, \quad (5)$$

where D is the Earth-Sun distance and dN_ν/dE is the spectral energy distribution of the final-state neutrinos and anti-neutrinos produced as a result of DM annihilation. This means that using the measured flux of neutrinos and the assumed DM annihilation spectra, we can constrain the annihilation rate under equilibrium [Eqs. (4) and (5)], and therefore, the DM-proton cross section.

We consider DM annihilation via three different channels: $b\bar{b}$, $\tau\bar{\tau}$ and $\nu\bar{\nu}$. The annihilation spectra are modeled using WIMPSIM [31,47], while the neutrino interactions in

the detector are simulated using GENIE [48]. At any given energy, we can weight the simulations by a desired flux model to calculate the total signal or background weights. The signal weight at a given energy is computed using the all-flavor neutrino spectrum from WIMPSIM for a given DM mass and channel, whereas the background weights are obtained from the atmospheric neutrino spectrum [49]. The signal PDF generation is a two-step process. First, for each annihilation channel and WIMP mass we determine an optimal range in reconstructed neutrino energy that maximizes the ratio of the summed signal weights and the square root of the background weights. Table I lists the optimal reconstructed neutrino energy ranges for each mass and annihilation channel. In the second step, we obtain the signal PDF by weighting the angular separation between the simulated neutrino and the reconstructed neutrino by the WIMPSIM flux at the given reconstructed neutrino energy. This procedure effectively assigns a higher weight to the neutrinos in the optimized energy range and a directional correlation with the Sun. Figure 1 (left panel) illustrates the signal and background PDFs as a function of the angular separation from the Sun.

2. Background estimation

The background PDFs are parametrized as a function of the angular separation from the Sun. For every event in the data, 30 azimuth angles are randomly sampled from a uniform distribution. These 30 angles are then combined with the Sun zenith angle to generate a random “fake” Sun position vector. The angle between the reconstructed neutrino direction and the randomized Sun direction is then used to fill the background PDF histogram. This process ensures that for any given position of the Sun, the background is estimated by randomizing the event directions with respect to the trajectory of the Sun (Fig. 1).

IV. RESULTS

For all three annihilation channels, and DM masses between 5 GeV and 100 GeV (up to 500 GeV for cross-checks), we determine the best-fit number of signal event, n_s , that maximizes the likelihood in Eq. (1). We obtain no statistically significant deviation from the expected background for any of the masses and channels we scanned. Figure 1 (right panel) shows the observed distribution of events in a 200° by 180° region in Sun-centered coordinates. The highest TS obtained for any test was 0.11 for a mass of 300 GeV with DM annihilating to $\tau^+\tau^-$. We note that such an underfluctuation of data across all tests we performed is not unlikely given that the tests are highly correlated. From background-only simulations, we expect all masses for a given channel to show a TS = 0, 5% of the time.

TABLE I. The reconstructed energy ranges of neutrinos used in the search for each WIMP mass and channel. The median energy of neutrinos in each range is shown in parentheses.

| WIMP Mass (GeV) | $\tau^+\tau^-$ E _{reco} (GeV) | $\nu\bar{\nu}$ E _{reco} (GeV) | $b\bar{b}$ E _{reco} (GeV) |
|--------------------|---|---|---------------------------------------|
| 5 | <9 (7) | 2–11 (8) | – |
| 10 | 1–16 (10) | <23 (13) | 0–11 (8) |
| 20 | 3–30 (15) | 13–39 (23) | <18 (11) |
| 35 | 8–50 (21) | 25–70 (38) | <27 (14) |
| 50 | 15–69 (29) | 42–86 (55) | 3–38 (17) |
| 100 | 30–128 (47) | 83–167 (107) | 6–70 (22) |

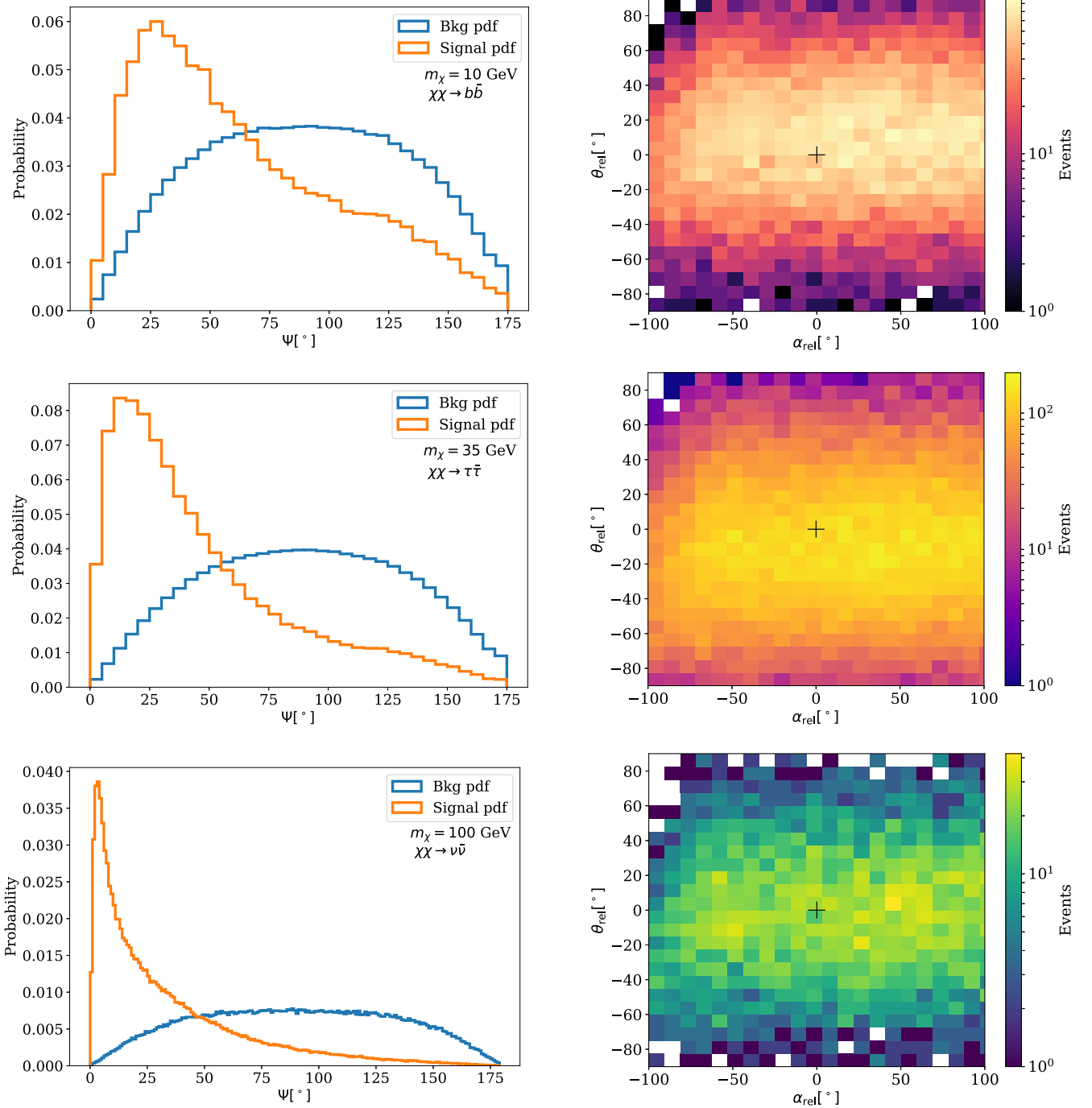


FIG. 1. Left: the PDF distributions for signal (orange) and background (blue) for three different annihilation channels and WIMP masses. The top panel corresponds to the $b\bar{b}$ annihilation channel for a 10 GeV WIMP mass, the middle panel to annihilation into $\tau^+\tau^-$ for 35 GeV WIMP mass, and the bottom panel annihilation into $\nu\bar{\nu}$ for 100 GeV WIMP mass, under the assumption of 100% annihilation to the respective channel. The angle Ψ represents the opening angle with respect to the Sun. Right: Sun-centered data maps for the corresponding channels (masses). The black cross marks the position of the Sun. α_{rel} and θ_{rel} are the azimuth and zenith angles relative to the Sun, respectively.

A. Systematic uncertainties

The results presented in this work are sensitive to systematic uncertainties due to detector effects. The systematic uncertainties affect the overall event rate, as

well as the angular and energy resolutions in the analysis. In order to study how these effects propagate into the signal PDFs and finally the upper limits on the DM-proton scattering cross section, we repeat all the analysis

TABLE II. The ratio of sensitivity (upper limits) obtained under different systematic variations to the baseline sensitivity (upper limits) obtained in this analysis. Absolute DOM efficiency and the uncertainties in the bulk ice scattering and absorption coefficients are the most dominant systematics in this analysis.

| WIMP Mass (GeV) | 10 | 20 | 35 | 50 | 100 |
|-----------------------|------|------|------|------|------|
| DOM Efficiency -6% | 1.17 | 1.13 | 1.10 | 1.09 | 1.03 |
| DOM Efficiency $+6\%$ | 0.85 | 0.90 | 0.96 | 0.95 | 0.97 |
| Absorption $+10\%$ | 1.06 | 1.05 | 1.03 | 1.02 | 0.97 |
| Scattering $+10\%$ | 1.02 | 1.06 | 1.08 | 1.09 | 1.06 |

steps on several simulated datasets. Each simulation was produced by varying the parameters of photon propagation at the detector, the DOM efficiency and the models of hole-ice (surrounding the strings) and the bulk ice (between the strings) up to $\pm 10\%$. We then compare the sensitivity obtained in these simulations to that obtained from the baseline case. Table II describes the effect on the sensitivity for each WIMP mass for the two most notable systematics, for annihilation to $b\bar{b}$ (other channels show similar trends). At low masses (10 GeV), the most dominant systematic—DOM efficiency [39]—degrades the sensitivity up to 20%. At 100 GeV, the biggest impact is due to the modeling of bulk ice properties, such as the scattering and absorption of photons by ice [50,51]. The effect is below 8%.

B. Constraints

We set 90% upper limits on n_s and the annihilation rate $\Gamma_{\text{ann}} [\text{s}^{-1}]$ of DM. The limits on annihilation rate are then converted to limits on the spin-dependent and spin-independent DM-proton cross sections following [52]. Tables III and IV summarize these results. Figure 2 shows the limits on the spin-dependent cross section as a function of DM mass. For each mass, we show the least constraining

TABLE IV. 90% C.L. limits on annihilation rate for DM annihilation to $b\bar{b}$ (left), $\tau^+\tau^-$ (center) and $\nu\bar{\nu}$.

| Mass (GeV) | $b\bar{b}$ $\Gamma_{\text{ann}} [\text{s}^{-1}] \times 10^{23}$ | $\tau\bar{\tau}$ $\Gamma_{\text{ann}} [\text{s}^{-1}] \times 10^{23}$ | $\nu\bar{\nu}$ $\Gamma_{\text{ann}} [\text{s}^{-1}] \times 10^{23}$ |
|------------|--|--|--|
| 5 | 139 | 9.55 | |
| 10 | 396 | 7.0 | 1.37 |
| 20 | 2.97 | 0.97 | 0.27 |
| 35 | 7.41 | 0.22 | 0.09 |
| 50 | 3.51 | 0.096 | 0.05 |
| 100 | 1.39 | 0.038 | 0.027 |

limits as obtained under the largest systematic variation for the respective mass (Table II). The differences between the limits for different channels depend on their spectral energy distributions relative to IceCube energy threshold. The differences between the limits for different masses are related to IceCube’s varying angular resolution with energy. In particular, poorer angular resolution ($\sim 35^\circ$) for neutrinos below ~ 10 GeV, results in an increased number of background events in the search region, worsening the limits for lower masses and softer channels. For any given channel, IceCube limits on the spin-dependent WIMP-proton cross section presented in this paper are world-leading and are the strictest so far among indirect DM search experiments. IceCube is particularly sensitive to direct annihilation of DM into neutrinos and the constraints for this channel are stronger than those obtained via direct detection [53].

The predicted flux of solar atmospheric neutrinos is, in principle, a background for dark matter searches from the Sun [55–57]. However, as shown in Ref. [58], IceCube is not yet sensitive enough to detect the expected flux of neutrinos from cosmic ray interactions in the Sun. In fact, compared to the sensitivity required [56,57], the cross section limits reported in this work are still nearly two orders of magnitude higher.

TABLE III. 90% C.L. limits on the spin-independent and spin-dependent dark matter-proton cross section for DM annihilation to $b\bar{b}$ (left), $\tau^+\tau^-$ (center) and $\nu\bar{\nu}$. The expected sensitivity from an ensemble of background-only observations is also shown under $\sigma_{\text{SD}}^{\text{Exp}} [\text{cm}^2]$ for each channel and DM mass.

| Mass (GeV) | $b\bar{b}$ | | | $\tau\bar{\tau}$ | | | $\nu\bar{\nu}$ | | |
|------------|--|--|---|--|--|---|--|--|---|
| | $\sigma_{\text{SI}} [\text{cm}^2] \times 10^{-41}$ | $\sigma_{\text{SD}} [\text{cm}^2] \times 10^{-39}$ | $\sigma_{\text{SD}}^{\text{Exp}} [\text{cm}^2] \times 10^{-39}$ | $\sigma_{\text{SI}} [\text{cm}^2] \times 10^{-41}$ | $\sigma_{\text{SD}} [\text{cm}^2] \times 10^{-39}$ | $\sigma_{\text{SD}}^{\text{Exp}} [\text{cm}^2] \times 10^{-39}$ | $\sigma_{\text{SI}} [\text{cm}^2] \times 10^{-41}$ | $\sigma_{\text{SD}} [\text{cm}^2] \times 10^{-39}$ | $\sigma_{\text{SD}}^{\text{Exp}} [\text{cm}^2] \times 10^{-39}$ |
| 5 | ... | ... | ... | 5.34 | 1.33 | 1.38 | 0.38 | 0.092 | 0.23 |
| 10 | 16.6 | 8.39 | 10.8 | 0.29 | 0.15 | 0.21 | 0.04 | 0.029 | 0.057 |
| 20 | 1.54 | 1.57 | 2.53 | 0.05 | 0.05 | 0.08 | 0.02 | 0.014 | 0.027 |
| 35 | 0.54 | 0.93 | 1.50 | 0.02 | 0.03 | 0.05 | 0.01 | 0.012 | 0.022 |
| 50 | 0.34 | 0.80 | 1.29 | 0.009 | 0.02 | 0.04 | 0.004 | 0.011 | 0.020 |
| 100 | 0.29 | 1.12 | 1.23 | 0.008 | 0.03 | 0.04 | 0.005 | 0.022 | 0.024 |

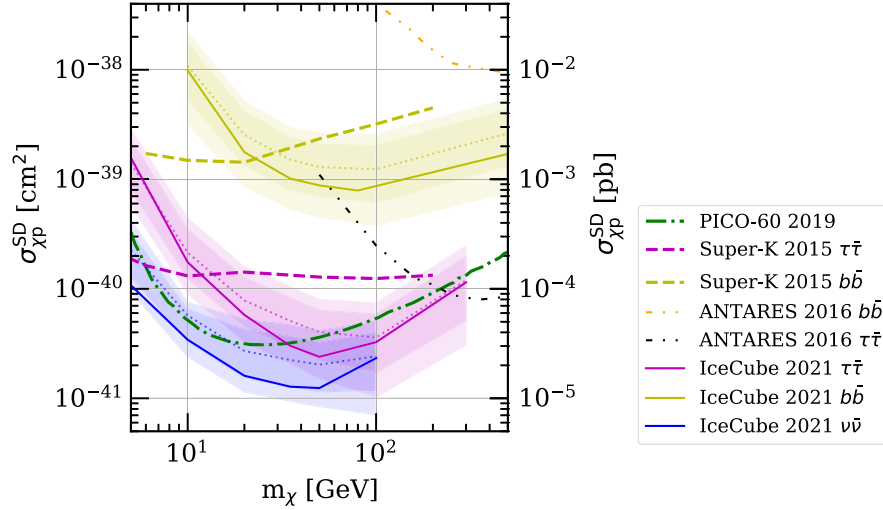


FIG. 2. 90% upper limits (solid lines) and expected sensitivity (dotted) on the spin-dependent cross section as a function of WIMP mass obtained by 7 years of IceCube DeepCore data in this work. We validated the analysis up to 500 GeV and 300 GeV for $b\bar{b}$ and $\tau^+\tau^-$ but only show up to 100 GeV in the tables for consistency. The dark and light shaded bands show the central 68% and 95% expected limits respectively. Also shown are limits from the Super-K [33], PICO-60 [53] and ANTARES [54] experiments.

V. CONCLUSION

We present a new analysis of low-energy neutrino data from the IceCube DeepCore detector to probe spin-dependent dark matter-proton scattering and dark matter annihilation rate in the Sun. Our limits are some of the strongest in the world for a range of dark matter masses between 5 GeV and 100 GeV. The work demonstrates that neutrino telescopes even with limited statistics and angular resolution at low-energies can still provide a powerful probe of new physics. The DM limits are also a powerful probe of the coupling constants of the nonrelativistic effective field theory of dark matter-nucleon interactions, including velocity- and momentum-dependent interactions [59].

ACKNOWLEDGMENTS

The IceCube Collaboration acknowledges the significant contributions to this manuscript from Garrett Neer and Mehr Un Nisa. USA—U.S. National Science Foundation-Office of Polar Programs, U.S. National Science Foundation-Physics Division, U.S. National Science Foundation-EPSCoR, Wisconsin Alumni Research Foundation, Center for High Throughput Computing (CHTC) at the University of Wisconsin—Madison, Open Science Grid (OSG), Extreme Science and Engineering Discovery Environment (XSEDE), Frontera computing project at the Texas Advanced Computing Center, U.S. Department of Energy-National

Energy Research Scientific Computing Center, Particle astrophysics research computing center at the University of Maryland, Institute for Cyber-Enabled Research at Michigan State University, and Astroparticle physics computational facility at Marquette University; Belgium—Funds for Scientific Research (FRS-FNRS and FWO), FWO Odysseus and Big Science programmes, and Belgian Federal Science Policy Office (Belspo), Germany—Bundesministerium für Bildung und Forschung (BMBF), Deutsche Forschungsgemeinschaft (DFG), Helmholtz Alliance for Astroparticle Physics (HAP), Initiative and Networking Fund of the Helmholtz Association, Deutsches Elektronen Synchrotron (DESY), and High Performance Computing cluster of the RWTH Aachen; Sweden—Swedish Research Council, Swedish Polar Research Secretariat, Swedish National Infrastructure for Computing (SNIC), and Knut and Alice Wallenberg Foundation; Australia—Australian Research Council; Canada—Natural Sciences and Engineering Research Council of Canada, Calcul Québec, Compute Ontario, Canada Foundation for Innovation, WestGrid, and Compute Canada; Denmark—Villum Fonden and Carlsberg Foundation; New Zealand—Marsden Fund; Japan—Japan Society for Promotion of Science (JSPS) and Institute for Global Prominent Research (IGPR) of Chiba University; Korea—National Research Foundation of Korea (NRF); Switzerland—Swiss National Science Foundation (SNSF); United Kingdom—Department of Physics, University of Oxford.

- [1] N. Aghanim *et al.* (Planck Collaboration), Planck 2018 results. VI. Cosmological parameters, *Astron. Astrophys.* **641**, A6 (2020).
- [2] K. Freese, Status of dark matter in the universe, *Int. J. Mod. Phys. D* **26**, 1730012–223 (2017).
- [3] G. Bertone, D. Hooper, and J. Silk, Particle dark matter: Evidence, candidates and constraints, *Phys. Rep.* **405**, 279 (2005).
- [4] M. R. Buckley and A. H. G. Peter, Gravitational probes of dark matter physics, *Phys. Rep.* **761**, 1 (2018).
- [5] W. H. Press and D. N. Spergel, Capture by the sun of a galactic population of weakly interacting, massive particles, *Astrophys. J.* **296**, 679 (1985).
- [6] A. H. G. Peter, Dark matter in the Solar System. II. WIMP annihilation rates in the Sun, *Phys. Rev. D* **79**, 103532 (2009).
- [7] M. Nisa, J. Beacom, A. Peter, R. Leane, T. Linden, K. Ng, and B. Zhou, The sun at GeV-TeV energies: A new laboratory for astroparticle physics, *Bull. Am. Astron. Soc.* **51**, 194 (2019), <https://baas.aas.org/pub/2020n3i194/release/1>.
- [8] M. Srednicki, K. A. Olive, and J. Silk, High-energy neutrinos from the sun and cold dark matter, *Nucl. Phys.* **B279**, 804 (1987).
- [9] J. Lundberg and J. Edsjö, Weakly interacting massive particle diffusion in the solar system including solar depletion and its effect on Earth capture rates, *Phys. Rev. D* **69**, 123505 (2004).
- [10] J. Conrad and O. Reimer, Indirect dark matter searches in gamma and cosmic rays, *Nat. Phys.* **13**, 224 (2017).
- [11] R. Garani and S. Palomares-Ruiz, Dark matter in the Sun: Scattering off electrons vs nucleons, *J. Cosmol. Astropart. Phys.* **05** (2017) 007.
- [12] C. Rott, T. Tanaka, and Y. Itow, Enhanced sensitivity to dark matter self-annihilations in the sun using neutrino spectral information, *J. Cosmol. Astropart. Phys.* **09** (2011) 029.
- [13] M. Ajello *et al.* (Fermi LAT Collaboration), Constraints on dark matter models from a Fermi LAT search for high-energy cosmic-ray electrons from the Sun, *Phys. Rev. D* **84**, 032007 (2011).
- [14] G. Wikström and J. Edsjö, Limits on the WIMP-nucleon scattering cross-section from neutrino telescopes, *J. Cosmol. Astropart. Phys.* **04** (2009) 009.
- [15] S. Ritz and D. Seckel, Detailed neutrino spectra from cold dark matter annihilations in the sun, *Nucl. Phys.* **B304**, 877 (1988).
- [16] K.-W. Ng, K. A. Olive, and M. Srednicki, Dark matter induced neutrinos from the sun: Theory versus experiment, *Phys. Lett. B* **188**, 138 (1987).
- [17] K. Belotsky, M. Khlopov, and C. Kouvaris, Muon flux limits for Majorana dark matter from strong coupling theories, *Phys. Rev. D* **79**, 083520 (2009).
- [18] S. Baum, L. Visinelli, K. Freese, and P. Stengel, Dark matter capture, subdominant WIMPs, and neutrino observatories, *Phys. Rev. D* **95**, 043007 (2017).
- [19] C. P. de los Heros, The quest for dark matter with neutrino telescopes, [arXiv:1511.03500](https://arxiv.org/abs/1511.03500).
- [20] L. Bergstrom, J. Edsjö, and P. Gondolo, Indirect detection of dark matter in km size neutrino telescopes, *Phys. Rev. D* **58**, 103519 (1998).
- [21] N. F. Bell and K. Petraki, Enhanced neutrino signals from dark matter annihilation in the Sun via metastable mediators, *J. Cosmol. Astropart. Phys.* **04** (2011) 003.
- [22] R. Allahverdi, Y. Gao, B. Knockel, and S. Shalgar, Indirect signals from solar dark matter annihilation to long-lived right-handed neutrinos, *Phys. Rev. D* **95**, 075001 (2017).
- [23] P. Meade, S. Nussinov, M. Papucci, and T. Volansky, Searches for long lived neutral particles, *J. High Energy Phys.* **06** (2010) 029.
- [24] B. Batell, M. Pospelov, A. Ritz, and Y. Shang, Solar gamma rays powered by secluded dark matter, *Phys. Rev. D* **81**, 075004 (2010).
- [25] P. Schuster, N. Toro, and I. Yavin, Terrestrial and solar limits on long-lived particles in a dark sector, *Phys. Rev. D* **81**, 016002 (2010).
- [26] J. L. Feng, J. Smolinsky, and P. Tanedo, Detecting dark matter through dark photons from the Sun: Charged particle signatures, *Phys. Rev. D* **93**, 115036 (2016).
- [27] R. K. Leane, K. C. Y. Ng, and J. F. Beacom, Powerful solar signatures of long-lived dark mediators, *Phys. Rev. D* **95**, 123016 (2017).
- [28] C. Arina, M. Backović, J. Heisig, and M. Lucente, Solar γ rays as a complementary probe of dark matter, *Phys. Rev. D* **96**, 063010 (2017).
- [29] J. Smolinsky and P. Tanedo, Dark photons from captured inelastic dark matter annihilation: Charged particle signatures, *Phys. Rev. D* **95**, 075015 (2017).
- [30] A. Albert *et al.* (HAWC Collaboration), Constraints on spin-dependent dark matter scattering with long-lived mediators from TeV observations of the sun with HAWC, *Phys. Rev. D* **98**, 123012 (2018).
- [31] C. Niblaeus, A. Beniwal, and J. Edsjö, Neutrinos and gamma rays from long-lived mediator decays in the Sun, *J. Cosmol. Astropart. Phys.* **11** (2019) 011.
- [32] M. N. Mazziotta, F. Loparco, D. Serini, A. Cuoco, P. De La Torre Luque, F. Gargano, and M. Gustafsson, Search for dark matter signatures in the gamma-ray emission towards the Sun with the Fermi Large Area Telescope, *Phys. Rev. D* **102**, 022003 (2020).
- [33] K. Choi *et al.* (Super-Kamiokande Collaboration), Search for Neutrinos from Annihilation of Captured Low-Mass Dark Matter Particles in the Sun by Super-Kamiokande, *Phys. Rev. Lett.* **114**, 141301 (2015).
- [34] M. G. Aartsen *et al.*, Search for annihilating dark matter in the Sun with 3 years of IceCube data, *Eur. Phys. J. C* **77**, 146 (2017).
- [35] M. Colom i Bernadich and C. Pérez de los Heros, Limits on Kaluza–Klein dark matter annihilation in the Sun from recent IceCube results, *Eur. Phys. J. C* **80**, 129 (2020).
- [36] S. Adrian-Martinez *et al.*, Limits on dark matter annihilation in the sun using the ANTARES neutrino telescope, *Phys. Lett. B* **759**, 69 (2016).
- [37] S. Adrián-Martínez *et al.* (ANTARES Collaboration), A search for Secluded Dark Matter in the Sun with the ANTARES neutrino telescope, *J. Cosmol. Astropart. Phys.* **05** (2016) 016.

- [38] R. K. Leane, T. R. Slatyer, J. F. Beacom, and K. C. Y. Ng, GeV-scale thermal wimps: Not even slightly ruled out, *Phys. Rev. D* **98**, 023016 (2018).
- [39] R. Abbasi *et al.* (IceCube Collaboration), Calibration and characterization of the IceCube photomultiplier tube, *Nucl. Instrum. Methods Phys. Res., Sect. A* **618**, 139 (2010).
- [40] R. Abbasi *et al.* (IceCube Collaboration), The design and performance of IceCube DeepCore, *Astropart. Phys.* **35**, 615 (2012).
- [41] M. Aartsen *et al.* (IceCube Collaboration), The IceCube neutrino observatory: Instrumentation and online systems, *J. Instrum.* **12**, P03012 (2017).
- [42] M. G. Aartsen *et al.* (IceCube Collaboration), Energy reconstruction methods in the IceCube neutrino telescope, *J. Instrum.* **9**, P03009 (2014).
- [43] M. G. Aartsen *et al.* (IceCube Collaboration), Measurement of Atmospheric Neutrino Oscillations at 6–56 GeV with IceCube Deepcore, *Phys. Rev. Lett.* **120**, 071801 (2018).
- [44] A. Gould, Weakly interacting massive particle distribution in and evaporation from the sun, *Astrophys. J.* **321**, 560 (1987).
- [45] R. Garani and S. Palomares-Ruiz, Evaporation of dark matter from celestial bodies, [arXiv:2104.12757](https://arxiv.org/abs/2104.12757).
- [46] A. Widmark, Thermalization time scales for WIMP capture by the Sun in effective theories, *J. Cosmol. Astropart. Phys.* **05** (2017) 046.
- [47] M. Blennow, J. Edsjo, and T. Ohlsson, Neutrinos from WIMP annihilations using a full three-flavor Monte Carlo, *J. Cosmol. Astropart. Phys.* **01** (2008) 021.
- [48] C. Andreopoulos *et al.*, The GENIE neutrino Monte Carlo generator, *Nucl. Instrum. Methods Phys. Res., Sect. A* **614**, 87 (2010).
- [49] M. Honda, T. Kajita, K. Kasahara, S. Midorikawa, and T. Sanuki, Calculation of atmospheric neutrino flux using the interaction model calibrated with atmospheric muon data, *Phys. Rev. D* **75**, 043006 (2007).
- [50] M. Ackermann *et al.*, Optical properties of deep glacial ice at the South Pole, *J. Geophys. Res.* **111**, D13203 (2006).
- [51] S. Fiedlschuster, The effect of hole ice on the propagation and detection of light in IceCube, [arXiv:1904.08422](https://arxiv.org/abs/1904.08422).
- [52] G. Jungman, M. Kamionkowski, and K. Griest, Supersymmetric dark matter, *Phys. Rep.* **267**, 195 (1996).
- [53] C. Amole *et al.* (PICO Collaboration), Dark matter search results from the complete exposure of the pico-60 C_3F_8 bubble chamber, *Phys. Rev. D* **100**, 022001 (2019).
- [54] S. Adrian-Martinez *et al.* (ANTARES Collaboration), Limits on dark matter annihilation in the sun using the ANTARES neutrino telescope, *Phys. Lett. B* **759**, 69 (2016).
- [55] J. Edsjo, J. Elevant, R. Enberg, and C. Niblaeus, Neutrinos from cosmic ray interactions in the Sun, *J. Cosmol. Astropart. Phys.* **06** (2017) 033.
- [56] C. A. Argüelles, G. de Wasseige, A. Fedynitch, and B. J. P. Jones, Solar atmospheric neutrinos and the sensitivity floor for solar dark matter annihilation searches, *J. Cosmol. Astropart. Phys.* **07** (2017) 024.
- [57] K. C. Y. Ng, J. F. Beacom, A. H. G. Peter, and C. Rott, Solar atmospheric neutrinos: A new neutrino floor for dark matter searches, *Phys. Rev. D* **96**, 103006 (2017).
- [58] M. Aartsen *et al.*, Searches for neutrinos from cosmic-ray interactions in the sun using seven years of IceCube data, *J. Cosmol. Astropart. Phys.* **02** (2021) 025.
- [59] L. Peters, K. Choi, and M. U. Nisa (IceCube), Constraining non-standard dark matter-nucleon interactions with IceCube, *Proc. Sci., ICRC2021* (2021) 522 [[arXiv:2108.05203](https://arxiv.org/abs/2108.05203)].